LAB1 Report

Pin-Jing, Li (111511015 *ouo.ee11@nycu.edu.tw*)
Jing-Kai, Huang
Duan-Kai, Wu

September 14, 2025

In lab 1 We explored the basic configuration of e^2 studio, ultrasound module and the basic signal processing flow of the wireless transmitted signal.

1 Hardware configuration

2 Error Source Analysis

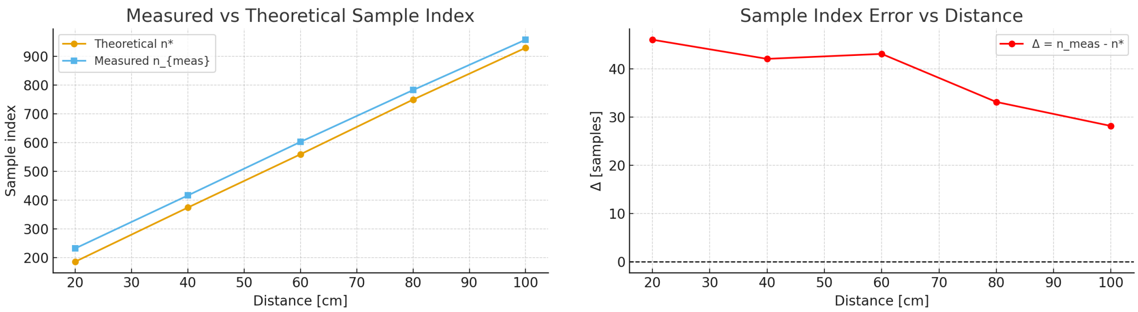

(a) Measured Peak and the theoretical sample (T=25)

(b) Error vs. distance

Figure 1: Comparing robust and non-robust design for linear precoder

We inspect the relative distance We retrieve back n_{meas} by aligning the starting sample by the maximum

Pair (cm)	n^*_{theory}	n_{meas}	$\Delta n^*_{\text{theory}}$	Δn_{meas}	$\frac{\Delta n_{\text{meas}}}{\Delta n^*_{\text{theory}}}$	Relative Error (%)
20→40	184.97→369.94	231→412	184.97	181	0.979	-2.1
40→60	369.94→554.91	412→598	184.97	186	1.006	+0.6
60→80	554.91→739.88	598→773	184.97	175	0.946	-5.4
80→100	739.88→924.86	773→953	184.97	180	0.973	-2.7

Table 1: Relative Distance Comparison (Measured vs. Theoretical)

Tx data

3 Signal Processing

some discussion below:

- **Correct "Detection" threshold.** The physically correct measure of the time of flight (TOF) would be the *wavefront* of the received signal.

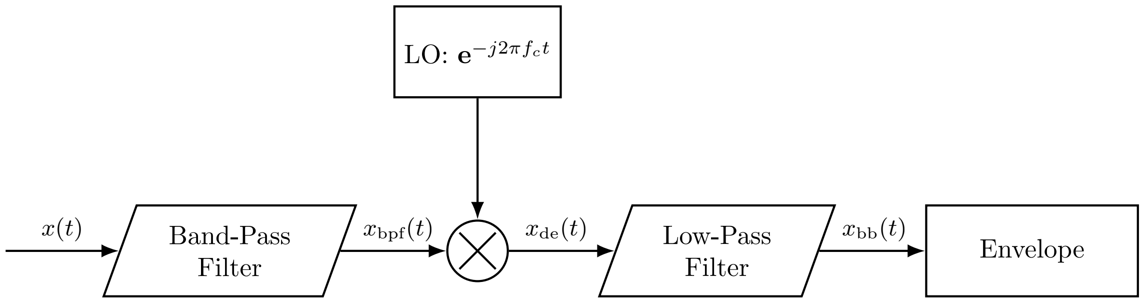

Figure 2: block diagram: signal → BPF → demod (mixer) → LPF → envelope.

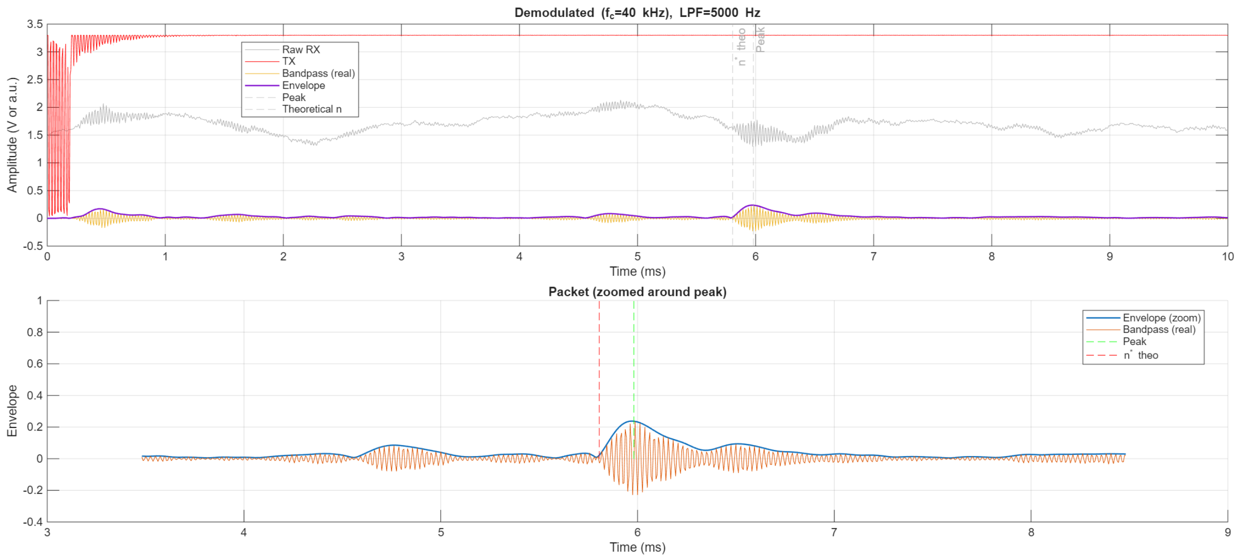

Figure 3: Time domain signal before and after filtering & demodulation

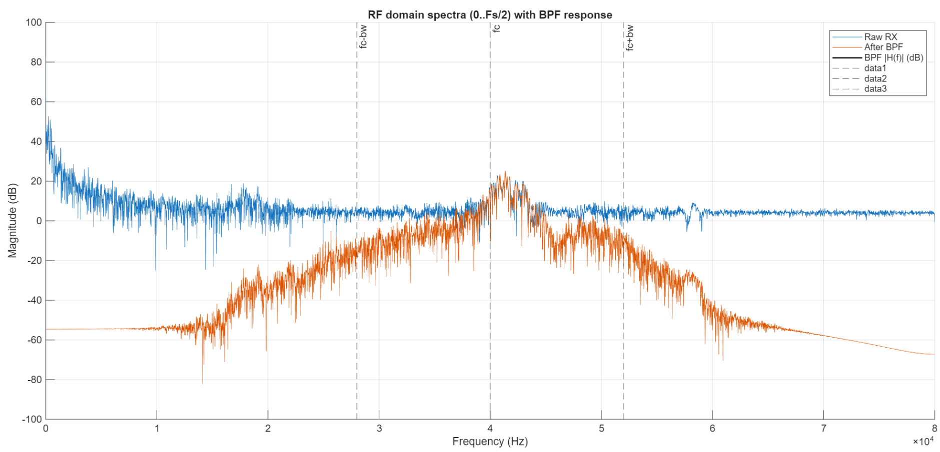

Figure 4: bpf

Bandpass Filtering

Given the sampled received signal $x(t)$, we first apply a bandpass filter to isolate the signal components near the carrier frequency. The bandpass-filtered signal is

$$x_{\text{bpf}}(t) = x(t) * h_{\text{bpf}}(t) \tag{1}$$

where $*$ denotes convolution and $h_{\text{bpf}}(t)$ is the impulse response of the bandpass filter.

Filter Design. We choose a 6^{th}-order IIR Butterworth bandpass filter with half-power frequencies

$$f_{\text{bp},1} = f_c - 2f_w, \qquad f_{\text{bp},2} = f_c + 2f_w,$$

where the carrier frequency $f_c = 40$ kHz and the signal bandwidth is

$$f_w = \frac{1}{T_{\text{burst}}} \approx 5 \text{ kHz}.$$

To ensure the filter design remains within valid frequency bounds, we compute:

$$\begin{aligned}
\texttt{bp_bw} &= \max\bigl(2f_w,\ 12 \text{ kHz}\bigr), \\
\texttt{bp_f1} &= \max\bigl(10,\ f_c - \texttt{bp_bw}\bigr), \\
\texttt{bp_f2} &= \min\bigl(\tfrac{F_s}{2} - 10,\ f_c + \texttt{bp_bw}\bigr),
\end{aligned}$$

where F_s is the sampling frequency.

MATLAB Implementation. The filter is implemented and applied using MATLAB as follows:

```
bp_bw = max(2*fw, 12e3); % Bandwidth selection
bp_f1 = max(10, fc - bp_bw); % Lower cutoff frequency
bp_f2 = min(Fs/2-10, fc + bp_bw); % Upper cutoff frequency

dbp = designfilt('bandpassiir','FilterOrder',6, ...
    'HalfPowerFrequency1', bp_f1, ...
    'HalfPowerFrequency2', bp_f2, ...
    'SampleRate', Fs);

rx_bp = filtfilt(dbp, rx_dc); % Zero-phase filtering
```

This produces the zero-phase bandpass-filtered signal $x_{\text{bpf}}(t)$.

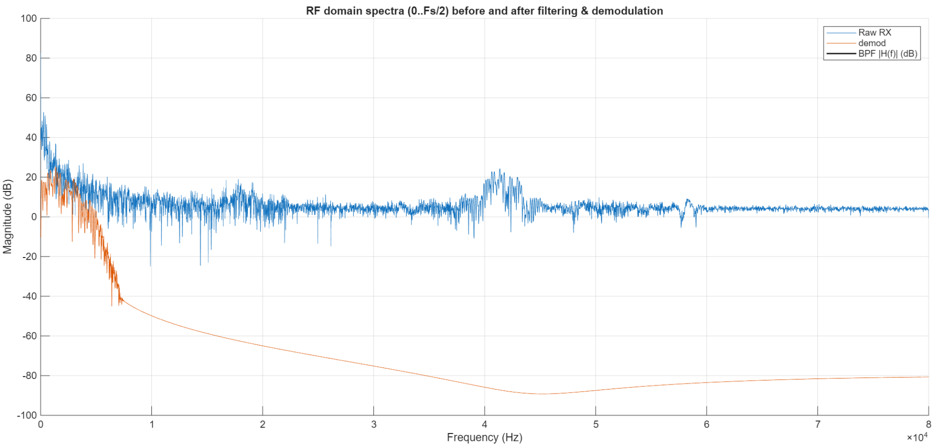

Figure 5: demod

References

[1] C.-Y. Chang and C.C. Fung, "Sparsity enhanced mismatch model for robust spatial intercell interference cancelation in heterogeneous networks," *IEEE Trans. on Communications*, vol. 63(1), pp. 125-139, Jan. 2015.

[2] I. P. Roberts, Y. Zhang, T. Osman, and A. Alkhateeb, "Real-world evaluation of full-duplex millimeter wave communication systems," *IEEE Trans. Wireless Commun.*, early access, Mar. 2024.

[3] K. Shen and W. Yu, "Fractional Programming for Communication Systems—Part I: Power Control and Beamforming," *IEEE Transactions on Signal Processing*, vol. 66, no. 10, pp. 2616-2630, May 15, 2018, doi: 10.1109/TSP.2018.2812733.

[4] J. Ho, A. Jain, and P. Abbeel, "Denoising diffusion probabilistic models," *Advances in Neural Information Processing Systems*, vol. 33, pp. 6840–6851, 2020.

[5] T. O'Shea and J. Hoydis, "An introduction to deep learning for the physical layer," *IEEE Transactions on Cognitive Communications and Networking*, vol. 3, no. 4, pp. 563–575, 2017.

[6] M. Servetnyk and C. C. Fung, "Distributed fronthaul-constrained joint transmission design and selection using augmented consensus-based dual decomposition," *Journal of Communications and Networks*, vol. 24, no. 4, pp. 419–437, Aug. 2022, doi: 10.23919/JCN.2022.000030.